Research Gate: Pharmaceutical Sciences, 15 (3) (2026) 31-37
ISSN – 2319-6831 (0nline)

Research Gate: Pharmaceutical Sciences
www.iresearchonline.com

Formulation and Evaluation of Emulgel Containing *Wrightia tinctoria* Leaves Extract for the Management of Psoriasis

Afsarmohamed. H * and P. Shanthi

K.M. College of Pharmacy, The Tamil Nadu Dr. M.G.R. Medical University, Chennai, Tamil Nadu, India.

ARTICLE INFO

Keywords:
Wrightia tinctoria
Emulgel
Psoriasis
Carbopol 934
Eugenol
Ex-vivo permeation
Molecular docking

Article History:
Received : 11th September 2026
Accepted : 12th September 2026
Available online : 12th September 2026

ABSTRACT

Psoriasis is a chronic, immune-mediated inflammatory skin disorder affecting roughly 2–3% of the world's population, and current mainstay therapies — corticosteroids, vitamin-D analogues, coal tar and biologics — remain limited by cutaneous adverse effects, tachyphylaxis and poor long-term adherence. *Wrightia tinctoria*, a plant long used in Siddha and Ayurvedic practice for psoriasis-like dermatoses, is presently available mainly as oil-based preparations that are greasy, staining and poorly controlled in their drug release. This study formulated and characterized a Carbopol 934 emulgel of W. tinctoria leaf hexane extract as a non-greasy alternative. Shade-dried leaves were Soxhlet-extracted in n-hexane, and the extract was profiled by GC-MS, which resolved 152 constituents; squalene (10.57%), β-caryophyllene (6.21%), eugenol (4.54%) and α-humulene (1.93%) were the major bioactives, with eugenol selected as the UV marker for quantitation (283 nm; Y = 0.01695X + 0.00270, R^2 = 0.99921). Five batches (F1–F5) were prepared by a traditional trial-batch method varying Carbopol 934 and Tween 80, and evaluated for pH, viscosity, spreadability, drug content, washability and centrifugation stability. Batch F3 (1.0 g Carbopol 934, 1.0 g Tween 80) combined a balanced viscosity (61,100 ± 600 cP), suitable pH (6.95 ± 0.01) and spreadability (6.15 ± 0.05 cm) with the most complete ex vivo permeation across excised goat skin (97.54 ± 2.34% at 10 h), following Korsmeyer–Peppas kinetics (R^2 = 0.9993, n = 0.8865) indicative of anomalous, non-Fickian transport. ATR-FTIR spectra of the extract and the finished F3 gel showed no unexplained new peaks, supporting drug–excipient compatibility. Molecular docking of the four major GC-MS-identified constituents against COX-2 (PDB 5KIR) and IL-17A (PDB 4HR9) showed squalene binding IL-17A most favourably (−8.053 kcal/mol), with humulene, caryophyllene and eugenol also showing appreciable COX-2 affinity, offering an in-silico mechanistic rationale consistent with the plant's traditional antipsoriatic use. Together, these findings support the optimized F3 emulgel as a reproducible, mechanistically plausible, non-greasy topical candidate for further preclinical development in psoriasis management.

INTRODUCTION

Psoriasis is a chronic, immune-mediated inflammatory dermatosis driven principally by a dysregulated Th17/IL-17 axis, producing erythematous, scaly plaques that considerably impair quality of life and affect an estimated 2–3% of the global population [1,2]. The disease's chronic, relapsing course, combined with the adverse-effect burden, tachyphylaxis and poor long-term compliance associated with corticosteroids, vitamin-D analogues, coal tar and biologic therapies, continues to drive interest in better-tolerated topical alternatives [3,4]. Keratinocyte amplification of the interleukin-23/Th17 pathway is now well established as a central driver of plaque formation, providing clear molecular targets — including IL-17A and the cyclo-oxygenase-2 (COX-2) inflammatory pathway — against which candidate therapeutics, including phytochemicals, can be rationally screened [5,6]. Both the immunologic drivers of this axis and the substantial comorbidity burden it produces have since been extensively reviewed [7,8].

Herbal alternatives have attracted renewed pharmaceutical interest as adjuncts or alternatives to conventional antipsoriatic therapy, on the basis of generally favourable tolerability and, in several cases, documented anti-inflammatory activity [9,10]. *Wrightia tinctoria* (family Apocynaceae) is one such plant, with a long history of use in Siddha and Ayurvedic medicine for psoriasis and related inflammatory dermatoses [11]. Prior pharmacological work has demonstrated reversal of parakeratosis in the mouse-tail model, clinical improvement in psoriasis vulgaris with proprietary W. tinctoria formulations, and systems-pharmacology evidence for a multi-target mechanism of action consistent with its traditional use [12–15]. However, the marketed and experimental preparations of W. tinctoria described to date are predominantly oil-based, and share the practical limitations common to oily topical vehicles: greasiness, staining of clothing, poor patient acceptability and largely uncontrolled drug release [11].

* Corresponding author
✉: H. AfsarMohamed: afsarstrom.01@gmail.com

Emulgels — biphasic emulsion systems structured within a hydrophilic gel network — combine the drug-loading capacity of an emulsion for lipophilic actives with the non-greasy feel, spreadability and controlled-release behaviour of a gel, and have been used successfully to reformulate lipophilic actives, including other essential-oil and terpenoid-rich extracts, for topical delivery [16,17]. Carbopol 934-based emulgels in particular have been reported for a range of poorly water-soluble actives, offering tunable viscosity and drug release through variation of the gelling agent and emulsifier concentrations [18,19]. A Carbopol emulgel therefore presents a rational vehicle for reformulating W. tinctoria leaf extract into a non-greasy, controlled-release topical system, addressing the principal limitation of existing oil-based preparations while retaining the phytochemical basis for its traditional antipsoriatic use.

The present study formulated and evaluated a Carbopol 934 emulgel containing W. tinctoria leaf hexane extract, prepared by a traditional trial-batch method varying Carbopol 934 and Tween 80 concentration. The extract was characterized by GC-MS to identify its major bioactive constituents and to select a suitable UV marker for quantitation; the resulting formulations were evaluated for physicochemical quality, drug–excipient compatibility by FTIR, ex vivo permeation across excised skin, and release-kinetic behaviour; and the major GC-MS-identified constituents were subjected to molecular docking against COX-2 and IL-17A to provide an in-silico mechanistic rationale for the traditional antipsoriatic use of the plant.

MATERIALS AND METHODS

Plant Material and Authentication

Fresh *Wrightia tinctoria* leaves were collected in Madurai, Tamil Nadu, and authenticated by a qualified botanist (Department of Botany, The American College, Madurai). A voucher specimen was retained for reference.

Figure 1. Photograph of Wrightia tinctoria flowers (authenticated plant material).

Extraction

Authenticated leaves were shade-dried for 7–10 days at 25–30 °C, powdered and passed through a 40-mesh sieve. The powder was extracted by continuous hot Soxhlet extraction using n-hexane (b.p. 68–69 °C) for 8 h. The solvent was allowed to evaporate under ambient conditions to yield a semi-solid, dark greenish extract, which was stored at 4 °C in an amber container until further use [20].

GC-MS Phytochemical Profiling

The hexane extract was analysed on a Thermo Trace GC/DSQ system (SGE-BPX5 fused-silica capillary column; helium carrier gas, 1 mL/min; electron ionisation, 70 eV; oven programme 50 °C → 150 °C at 3 °C/min, held 10 min, → 250 °C at 10 °C/min) at the School of Chemistry, Madurai Kamaraj University. Peaks were identified against the NIST 2020 and Wiley 7N mass-spectral libraries, accepting matches with a similarity index ≥ 80%.

UV Calibration of Eugenol

Eugenol, the selected UV marker compound, was quantified at its λmax (283 nm) on a Shimadzu UV-1800 spectrophotometer. A calibration series (2–10 µg/mL) was prepared and read in triplicate, and the calibration equation was derived by linear regression, validated per ICH Q2(R2) [21,22].

Formulation Development

Five emulgel batches (F1–F5) were prepared by a traditional (conventional) trial-batch method, varying Carbopol 934 (gelling agent) and Tween 80 (hydrophilic emulsifier) concentration across low, intermediate and high levels, identified from preliminary trials as the two variables exerting the dominant influence on viscosity, spreadability and drug release (Table 1) [18,23]. Briefly, Carbopol 934 was hydrated in purified water and neutralised with triethanolamine to form the gel base; the extract was dissolved in liquid paraffin with Span 80 as the oil phase, Tween 80 was dispersed in the aqueous phase, and the resulting emulsion was incorporated into the gel base in a 1:1 ratio under continuous stirring to yield the finished emulgel.

Table 1. Formulation Variables and Batch Composition (F1–F5)

Batch	Carbopol 934 (g)	Tween 80 (g)	W.T. extract (g)	Liquid paraffin (g)	Purified water q.s. (g)
F1	0.5	1.0	2.0	5.0	100
F2	1.5	0.5	2.0	5.0	100
F3 (optimized)	**1.0**	**1.0**	**2.0**	**5.0**	**100**
F4	0.5	1.5	2.0	5.0	100
F5	1.5	1.5	2.0	5.0	100

Values are per 100 g batch. Composition reflects the two independently varied formulation variables (Carbopol 934, Tween 80); remaining excipients (methylparaben, propylparaben, propylene glycol) were held constant across batches.

Evaluation of Physicochemical Parameters

All batches were evaluated in triplicate (n = 3, mean ± SD) for physical appearance and homogeneity, pH (digital pH meter), viscosity (viscometer), spreadability (parallel-plate method), eugenol-equivalent drug content (UV

spectrophotometry, back-calculated from the calibration equation of Section 2.4), washability, and centrifugation stability.

FTIR Drug–Excipient Compatibility

ATR-FTIR spectra (4000–650 cm^{-1}, 4 cm^{-1} resolution; JASCO spectrometer) were recorded for the raw hexane extract and for the optimized F3 gel, and the two spectra were compared for the appearance of new absorption bands or unexplained peak shifts indicative of chemical interaction.

***Ex Vivo* Permeation Study**

Cumulative percentage permeation of all five batches was determined across excised goat skin over 10 h using a modified diffusion-cell assembly (phosphate buffer pH 7.4 receptor, sink conditions, 37 ± 0.5 °C), with hourly sampling and UV back-calculation of eugenol-equivalent permeated concentration [24].

Release-Kinetic Modelling

Cumulative permeation data for all batches were fitted to zero-order, first-order, Higuchi, Korsmeyer–Peppas, Hixson–Crowell and Weibull models to identify the best-fit release mechanism for each formulation [25,26].

Molecular Docking

The four major GC-MS-identified constituents (squalene, β-caryophyllene, eugenol, α-humulene) were docked against COX-2 (PDB 5KIR) and IL-17A (PDB 4HR9), retrieved from the RCSB Protein Data Bank [27], using Attracting Cavities 2.0 (SP-dG scoring) and, for eugenol, AutoDock Vina (binding affinity scoring) [28]. Because SP-dG and Vina-affinity values derive from different scoring algorithms, they were interpreted independently within each method rather than compared numerically across methods.

Statistical Analysis

All quantitative results are expressed as mean ± standard deviation (SD) of triplicate determinations (n = 3). Batch comparisons were made descriptively across the five trial batches, consistent with the traditional (non-statistical-design) trial-batch approach used for formulation development.

RESULTS AND DISCUSSION

Extraction and GC-MS Phytochemical Profile

Soxhlet hexane extraction yielded a homogeneous, dark greenish, semi-solid extract that remained physically stable on storage with no phase separation or crystallisation. GC-MS analysis of the extract resolved 152 constituent peaks (NIST 2020/Wiley 7N library match, similarity index ≥ 80%) (Figure 2). Squalene (10.57% relative area), β-caryophyllene (6.21%), eugenol (4.54%) and α-humulene (1.93%) were selected as the major bioactive constituents for further study, together accounting for approximately 23% of total resolved peak area (Table 2), consistent with the chemically heterogeneous, lipophilic character typical of hexane-soluble terpenoid-rich plant extracts.

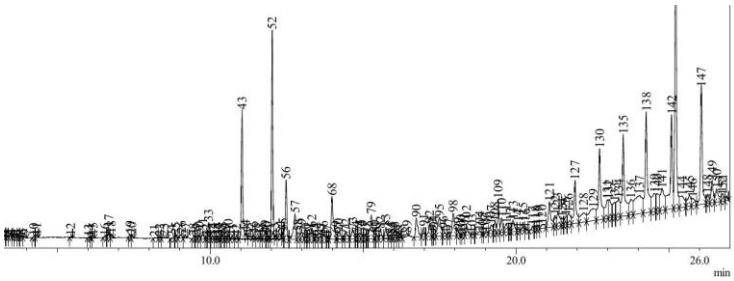

Figure 2. GC-MS total ion chromatogram of the Wrightia tinctoria hexane extract.

Table 2. Major Bioactive Constituents Identified by GC-MS

Compound	RT (min)	Area (%)	Formula / MW	Reported relevance
Squalene	25.220	10.57	C30H50, 410	Barrier repair; IL-17A affinity (this study)
β-Caryophyllene	12.030	6.21	C15H24, 204	CB2 agonist / NF-κB inhibitor
Eugenol	11.040	4.54	C10H12O2, 164	COX-2 inhibitor; UV marker
α-Humulene	12.485	1.93	C15H24, 204	COX-2 inhibitor; synergist with caryophyllene

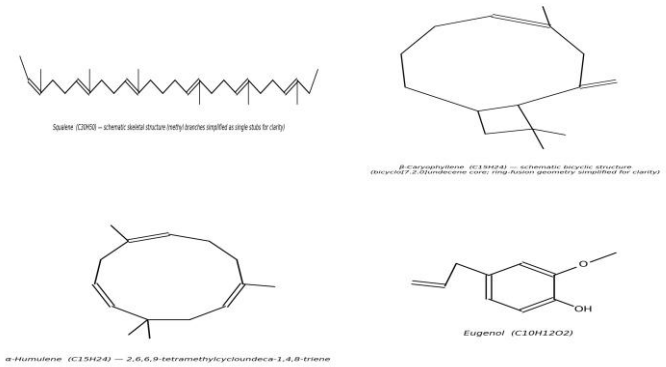

Figure 3. Chemical structures of the four major GC-MS-identified constituents: squalene, β-caryophyllene, α-humulene and eugenol.

UV Calibration of Eugenol

The eugenol calibration curve at 283 nm was linear over 2–10 µg/mL (Y = 0.01695X + 0.00270, R^2 = 0.99921), confirming suitability for back-calculation of eugenol-equivalent concentrations in the drug-content and permeation studies described below.

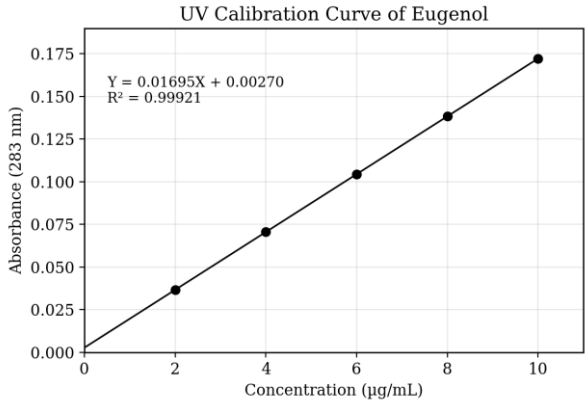

Figure 4. UV calibration curve of eugenol at 283 nm (2–10 µg/mL).

Physicochemical Evaluation of F1–F5

All batches showed pH in the range 6.78–7.08, acceptable for topical application, with no meaningful dependence on formulation composition. Viscosity, in contrast, tracked Carbopol 934 concentration closely, with the high-Carbopol batches F2 (77,200 ± 300 cP) and F5 (85,400 ± 500 cP) substantially more viscous than the low-Carbopol batches F1 (44,500 ± 400 cP) and F4 (31,200 ± 300 cP); F3 occupied an intermediate, balanced position (61,100 ± 600 cP). Spreadability varied inversely with viscosity, as expected for a shear-thinning semisolid, and eugenol-equivalent drug content was uniform across all batches (0.084–0.090 mg/100 mg, %CV ≤ 2.2%), confirming reproducible extract incorporation independent of the Carbopol:Tween 80 ratio (Table 3).

Table 3. Physicochemical Evaluation of Formulations F1–F5 (Mean ± SD, n = 3)

Parameter	F1	F2	F3 (optimized)	F4	F5
pH	6.81 ± 0.01	7.02 ± 0.01	6.95 ± 0.01	6.78 ± 0.01	7.08 ± 0.01
Viscosity (cP)	44,500 ± 400	77,200 ± 300	61,100 ± 600	31,200 ± 300	85,400 ± 500
Spreadability (cm)	7.65 ± 0.15	4.85 ± 0.05	6.15 ± 0.05	8.42 ± 0.08	3.90 ± 0.05
Drug content (mg/100 mg)	0.084 ± 0.0003	0.090 ± 0.0018	0.088 ± 0.0019	0.087 ± 0.0015	0.090 ± 0.0012
Washability (s)	8.0 ± 0.5	22.0 ± 1.3	14.3 ± 0.6	5.0 ± 0.3	34.0 ± 2.0

Figure 5. Photographs of the formulated batches F1–F5, showing the visual gradient in colour and consistency across the Carbopol 934:Tween 80 series (F3, centre, is the optimized batch).

FTIR Drug–Excipient Compatibility

The extract's principal absorption bands (O–H stretch, 3414 cm^{-1}; C–H asymmetric/symmetric stretch, 2923/2853 cm^{-1}; ester C=O stretch, 1735 cm^{-1}; C–O–C stretch, 1244/1170 cm^{-1}) were compared against the finished F3 gel spectrum. The aliphatic/terpenoid C–H bands were retained essentially unshifted ($\Delta \approx 1$ cm^{-1}), confirming that the extract's core hydrocarbon backbone survives formulation processing intact. The O–H band broadened and shifted (3414 → 3347 cm^{-1}), attributable to superimposition with the Carbopol gel base's own hydrogen-bonded O–H network rather than chemical incompatibility, and the extract's ester carbonyl band was not separately resolved, being masked by the broad Carbopol carbonyl/water-bending envelope at 1640 cm^{-1} — an expected dilution effect given the extract's low (2% w/w) loading. No new, unexplained absorption peaks were observed in the F3 spectrum, supporting drug–excipient compatibility.

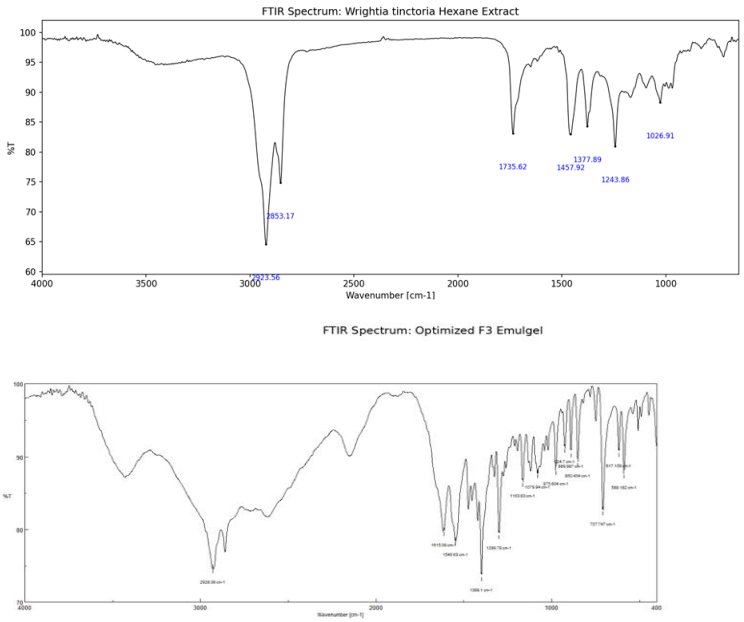

Figure 6. FTIR spectra of (a) the Wrightia tinctoria hexane extract and (b) the optimized F3 emulgel.

Ex-Vivo Permeation and Selection of the Optimized Batch

F3 achieved the highest and most progressive 10-h cumulative permeation (97.54 ± 2.34%), followed by F5 (87.50%), F1 (78.99%), F4 (68.84%) and F2 (25.93%) (Table 4). F2 (high Carbopol, low Tween 80) showed markedly restricted release, consistent with a denser gel network limiting diffusion, while F4 (low Carbopol, high Tween 80) showed rapid early release consistent with a weaker gel matrix. Taken together with the physicochemical results, F3 was selected as the optimized formulation on the basis of its balanced viscosity, suitable pH, acceptable spreadability, uniform drug content, absence of phase separation on centrifugation, and — decisively — its superior and most complete permeation profile.

Table 4. Cumulative Percentage Permeation of F1–F5 Over 10 h (Mean, n = 3)

Time (h)	F1 (%)	F2 (%)	F3 (%)	F4 (%)	F5 (%)
2	31.87	8.48	33.34	23.53	39.86
4	56.90	15.91	59.90	43.53	65.54
6	69.51	20.89	79.89	56.93	78.06
8	76.32	24.23	90.45	64.54	84.84
10	78.99	25.93	97.54	68.84	87.50

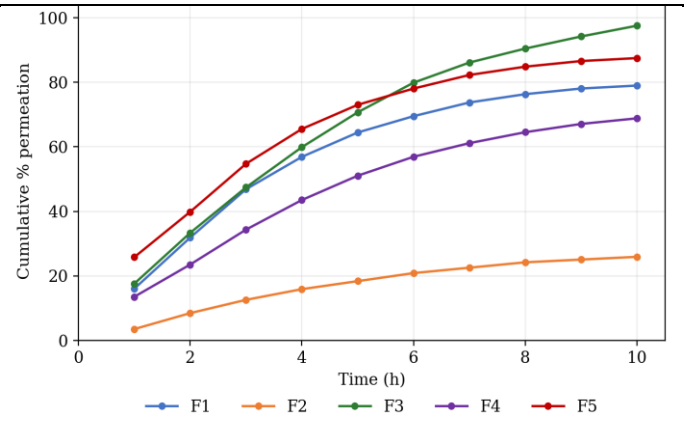

Figure 7. Comparative cumulative percentage permeation profiles of formulations F1–F5 across excised goat skin over 10 h.

Release-Kinetic Modelling

Fitting the six candidate models showed batch F3 best described by Korsmeyer–Peppas kinetics (R^2 = 0.9993; n = 0.8865), with a release exponent between 0.45 and 0.89 indicative of anomalous (non-Fickian) transport combining drug diffusion through, and relaxation/erosion of, the Carbopol gel network. F2 was best described by a Higuchi model (R^2 = 0.9711), consistent with predominantly diffusion-controlled release from its denser matrix, while F1, F4 and F5 also best fitted Korsmeyer–Peppas kinetics (Table 5), suggesting a broadly consistent, matrix-controlled release mechanism across the trial-batch series that is modulated, rather than fundamentally altered, by Carbopol:Tween 80 ratio.

Table 5. Best-Fit Release Kinetic Model Summary F1–F5

Formulation	Best-fit model	R^2	10-h release (%)
F1	Korsmeyer–Peppas	0.9961	78.99
F2	Higuchi	0.9711	25.93
F3 (optimized)	**Korsmeyer–Peppas**	**0.9993**	**97.54**
F4	Korsmeyer–Peppas	0.9964	68.84
F5	Korsmeyer–Peppas	0.9978	87.50

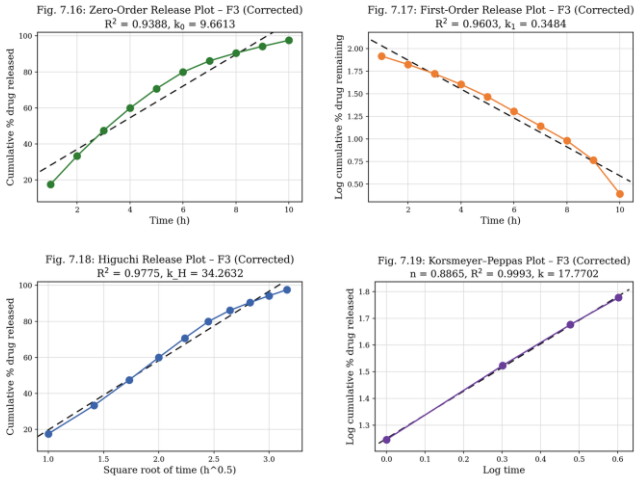

Figure 8. Release-kinetic model plots for the optimized formulation (F3): (a) zero-order, (b) first-order, (c) Higuchi, (d) Korsmeyer–Peppas.

Reproducibility of the Optimized Batch

Three independently prepared F3 batches showed consistent appearance, homogeneity and stability, with %CV below 3% for all key parameters (pH, viscosity, spreadability, drug content), confirming that the traditional trial-batch process yields a reproducible optimized formulation.

Molecular Docking of Major Bioactive Constituents

Molecular docking of the four major GC-MS-identified constituents against COX-2 (PDB 5KIR) and IL-17A (PDB 4HR9) showed squalene binding IL-17A most favourably (SP-dG = −8.053 kcal/mol), with α-humulene (−6.734 kcal/mol) and β-caryophyllene (−6.597 kcal/mol) showing appreciable COX-2 affinity by the same scoring method, and eugenol showing moderate COX-2 affinity by AutoDock Vina (−5.312 kcal/mol) (Table 6). Decomposition of the Attracting-Cavities-docked ligands' binding free energy showed the interaction dominated by nonpolar (hydrophobic) contributions for all three terpenoid ligands, consistent with their lipophilic, largely hydrocarbon structures. These docking-predicted affinities are consistent with independently reported

bioactivity for each ligand: squalene/squalane has been shown to counteract UVA-induced oxidative stress and COX-2/NF-κB upregulation and to support dermal wound repair [29], β-caryophyllene shows favourable skin permeation correlated with in vivo antiedematogenic activity from topical nanoemulgel vehicles [30], and α-humulene dose-dependently suppresses pro-inflammatory interleukin-6 release in lipopolysaccharide-stimulated macrophages [31]. Taken together, these in-silico findings, while not a substitute for direct pharmacodynamic or clinical evidence, provide a plausible dual-target (COX-2/IL-17A) mechanistic rationale consistent with the traditional antipsoriatic use of W. tinctoria and with the Th17/IL-17- and COX-2-mediated inflammatory pathways implicated in psoriasis pathogenesis.

Table 6. Molecular Docking Summary

Compound	Target (PDB ID)	Method	Best score (kcal/mol)
Squalene	IL-17A (4HR9)	Attracting Cavities 2.0	−8.053 (SP-dG)
α-Humulene	COX-2 (5KIR)	Attracting Cavities 2.0	−6.734 (SP-dG)
β-Caryophyllene	COX-2 (5KIR)	Attracting Cavities 2.0	−6.597 (SP-dG)
Eugenol	COX-2 (5KIR)	AutoDock Vina	−5.312 (affinity)

SP-dG (Attracting Cavities) and Vina affinity (eugenol) use different scoring algorithms and are not directly numerically comparable.

Comparison with Related Formulation Work

The release behaviour observed for F3 is broadly consistent with prior reports of eugenol-loaded gel systems: Rohmani et al. reported HPMC-gelling-agent-dependent in vitro eugenol release, and Akram et al. similarly demonstrated eugenol/linalool release from a polymeric emulgel governed by gel-matrix composition [32,33], supporting Carbopol/Tween 80 ratio as a key controllable release determinant in the present system as well. The permeation methodology and time-course sampling approach used here follow the general ex vivo transdermal evaluation framework described by Wahid et al. for a chitosan-modified transdermal system [34]. Together with the docking-supported dual-target rationale, these comparisons position the optimized W. tinctoria emulgel as methodologically consistent with, and mechanistically complementary to, existing phytochemical-loaded topical delivery literature for inflammatory dermatoses [35].

CONCLUSION

A Carbopol 934-based emulgel containing *Wrightia tinctoria* leaf hexane extract was successfully formulated by a traditional trial-batch method and optimized as batch F3, which combined balanced physicochemical properties with the most complete and reproducible ex vivo permeation (97.54% at 10 h, Korsmeyer–Peppas kinetics) among the five batches evaluated. FTIR analysis confirmed drug–excipient compatibility, and molecular docking of the major GC-MS-identified constituents against COX-2 and IL-17A provided an in-silico mechanistic rationale consistent with the plant's traditional antipsoriatic use, with squalene emerging as the strongest predicted IL-17A binder. These findings support the optimized emulgel as a non-greasy, controlled-release alternative to existing oil-based W. tinctoria preparations, warranting further in vitro bioassay and in vivo evaluation before clinical translation.

Acknowledgement:

Authors are thankful to K. M. College of Pharmacy, Madurai, Tamilnadu, India.

REFERENCES

1. Prausnitz MR, Langer R. Transdermal drug delivery. Nat Biotechnol. 2008;26:1261–1268. doi:10.1038/nbt.1504.
2. Leite-Silva VR, Almeida MM, Fradin A, Grice JE, Roberts MS. Delivery of drugs applied topically to the skin. Expert Rev Dermatol. 2012;7(4):383–397. doi:10.1586/edm.12.32.
3. Armstrong AW, Read C. Pathophysiology, clinical presentation, and treatment of psoriasis: a review. JAMA. 2020;323(19):1945–1960. doi:10.1001/jama.2020.4006.
4. Gu X, Wang X, Bin Y, Xue R, Zhu G. Global trends and future predictions of psoriasis burden: insights from the GBD 2021 study. Psoriasis (Auckl). 2025;15:1–14. doi:10.2147/PTT.S558419.
5. Lowes MA, Russell CB, Martin DA, Towne JE, Krueger JG. The IL-23/T17 pathogenic axis in psoriasis is amplified by keratinocyte responses. Trends Immunol. 2013;34(4):174–181. doi:10.1016/j.it.2012.11.005.
6. Nakajima K. Critical role of the interleukin-23/T-helper 17 cell axis in the pathogenesis of psoriasis. J Dermatol. 2012;39(3):219–224. doi:10.1111/j.1346-8138.2011.01458.x.
7. Blauvelt A, Chiricozzi A. The immunologic role of IL-17 in psoriasis and psoriatic arthritis pathogenesis. Clin Rev Allergy Immunol. 2018;55(3):379–390. doi:10.1007/s12016-018-8702-3.
8. Menter A, Krueger GG, Paek SY, Kivelevitch D, Adamopoulos IE, Langley RG. Interleukin-17 and interleukin-23: a narrative review of mechanisms of action in psoriasis and associated comorbidities. Dermatol Ther (Heidelb). 2021;11(2):385–400. doi:10.1007/s13555-021-00483-2.
9. Deng S, May BH, Zhang AL, Lu C, Xue CC. Plant extracts for the topical management of psoriasis: a systematic review and meta-analysis. Br J Dermatol. 2013;169(4):769–782. doi:10.1111/bjd.12403.
10. Gulliver W, Donsky HJ. A report on three recent clinical trials using Mahonia aquifolium 10% topical cream and a review of the worldwide clinical experience with Mahonia aquifolium for the treatment of plaque psoriasis. Am J Ther. 2005;12(5):398–406.
11. Srivastava R. A review on phytochemical, pharmacological, and pharmacognostical profile of *Wrightia tinctoria*: adulterant of kurchi. Pharmacogn Rev. 2014;8(15):36–44. doi:10.4103/0973-7847.125528.

12. Dhanabal SP, Baskar Anand Raj, Muruganantham N, Praveen TK, Raghu PS. Screening of *Wrightia tinctoria* leaves for anti-psoriatic activity. Hygeia J Drugs Med. 2012;4(1):73–78.
13. Mitra S, Seshadri S, Venkataranganna M, Gopumadhavan S. Reversal of parakeratosis, a feature of psoriasis, by *Wrightia tinctoria* (in emulsion) — histological evaluation based on mouse tail test. Indian J Dermatol. 1998;43:102–104.
14. Baktha Reddy NB. Clinical and histopathological evaluation of the effect of *Wrightia tinctoria* formulation (RegSoR®) on psoriasis vulgaris. US Dermatol Rev. 2007:6–8.
15. Sundarrajan S, Lulu S, Arumugam M. Deciphering the mechanism of action of *Wrightia tinctoria* for psoriasis based on a systems pharmacology approach. J Altern Complement Med. 2017;23(11):1–13.
16. Ajazuddin, Alexander A, Khichariya A, Gupta S, Patel RJ, Giri TK, Tripathi DK. Recent expansions in an emergent novel drug delivery technology: emulgel. J Control Release. 2013;171(2):122–132. doi:10.1016/j.jconrel.2013.06.030.
17. Dhawas V, Dhabarde D, Patil S. Emulgel: a comprehensive review for novel topical drug delivery system. Int J Recent Sci Res. 2020;11(04):38135–38136.
18. Khullar R, Kumar D, Seth N, Saini S. Formulation and evaluation of mefenamic acid emulgel for topical delivery. Saudi Pharm J. 2012;20(1):63–67.
19. Khan BA, Ali A, Hosny KM, Halwani AA, Almehmady AM, Iqbal M, Alharbi WS, Abualsunun WA, Bakhaidar RB, Murshid SSA, Khan MK. Carbopol emulgel loaded with ebastine for urticaria: development, characterization, in vitro and in vivo evaluation. Pharmaceutics. 2022;14(6):1201.
20. World Health Organization. Quality Control Methods for Herbal Materials. Geneva: World Health Organization; 2011. ISBN 9789241500739.
21. International Council for Harmonisation. ICH Q2(R2): Validation of Analytical Procedures. Geneva: ICH; 2024.
22. Rowe RC, Sheskey PJ, Quinn ME, editors. Handbook of Pharmaceutical Excipients. 6th ed. London: Pharmaceutical Press; 2009.
23. Taylor KMG, Aulton ME, editors. Aulton's Pharmaceutics: The Design and Manufacture of Medicines. 6th ed. Elsevier; 2022.
24. Mahmood S, Thakur A, Mirza MA, Bhatia A. Franz diffusion cell and its implication in skin permeation studies. J Dispersion Sci Technol. 2024;45(5):943–956. doi:10.1080/01932691.2023.2188923.
25. Higuchi T. Rate of release of medicaments from ointment bases containing drugs in suspension. J Pharm Sci. 1961;50(10):874–875. doi:10.1002/jps.2600501018.
26. Korsmeyer RW, Gurny R, Doelker E, Buri P, Peppas NA. Mechanisms of solute release from porous hydrophilic polymers. Int J Pharm. 1983;15(1):25–35. doi:10.1016/0378-5173(83)90064-9.
27. Berman HM, Westbrook J, Feng Z, Gilliland G, Bhat TN, Weissig H, Shindyalov IN, Bourne PE. The Protein Data Bank. Nucleic Acids Res. 2000;28(1):235–242. doi:10.1093/nar/28.1.235.
28. Trott O, Olson AJ. AutoDock Vina: improving the speed and accuracy of docking with a new scoring function, efficient optimization, and multithreading. J Comput Chem. 2010;31(2):455–461. doi:10.1002/jcc.21334.
29. Wolosik K, Chalecka M, Gasiewska G, Palka J, Surazynski A. Squalane as a promising agent protecting UV-induced inhibition of collagen biosynthesis and wound healing in human dermal fibroblast. Molecules. 2025;30(9):1964. doi:10.3390/molecules30091964.
30. Weimer P, Kreutz T, Limberger RP, Rossi RC, de Lima ÁAN, Veiga VF Jr, de Araújo BV, Koester LS. Correlation between the skin permeation profile of the synthetic sesquiterpene compounds, beta-caryophyllene and caryophyllene oxide, and the antiedematogenic activity by topical application of nanoemulgels. Biomolecules. 2022;12(8):1102. doi:10.3390/biom12081102.
31. Becker L, Holtmann D. Anti-inflammatory effects of α-humulene on the release of pro-inflammatory cytokines in lipopolysaccharide-induced THP-1 cells. Cell Biochem Biophys. 2024;82(2):839–847. doi:10.1007/s12013-024-01235-7.
32. Rohmani S, Yugatama A, Wijayanti I, Ermawati DE, Artanti AN, Kundarto W, Zulpadly MF. Characteristics of eugenol products and in vitro release in gel base with hydroxypropyl methylcellulose (HPMC) variant as gelling agent. Int J App Pharm. 2021;13(6):106–111. doi:10.22159/ijap.2021v13i6.42351.
33. Akram MA, Khan BA, Khan MK, Alqahtani A, Alshahrani SM, Hosny KM. Fabrication and characterization of polymeric pharmaceutical emulgel co-loaded with eugenol and linalool for the treatment of Trichophyton rubrum infections. Polymers. 2021;13(22):3904. doi:10.3390/polym13223904.
34. Wahid A, Sridhar BK, Shivakumar S. Preparation and evaluation of transdermal drug delivery system of etoricoxib using modified chitosan. Indian J Pharm Sci. 2008;70(4):455–460. doi:10.4103/0250-474X.44593.
35. Yadav T, Yadav HKS, Raizaday A, Alam MS. The treatment of psoriasis via herbal formulation and nano-polyherbal formulation: a new approach. BioImpacts. 2024;15(1):30341. doi:10.34172/bi.30341.